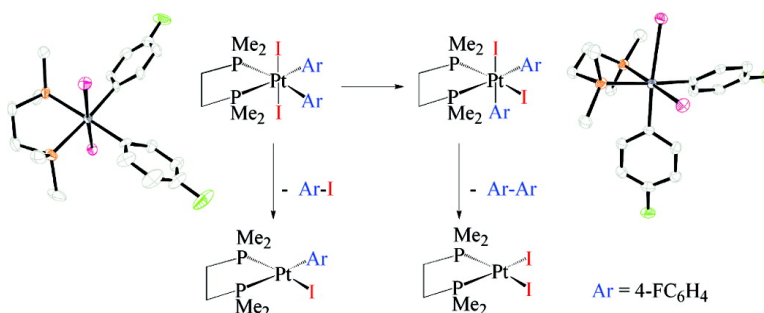


Competitive Aryl–Iodide vs Aryl–Aryl Reductive Elimination Reactions in Pt(IV) Complexes: Experimental and Theoretical Studies

Anette Yahav-Levi, Israel Goldberg, Arkadi Vigalok, and Andrei N. Vedernikov

J. Am. Chem. Soc., **2008**, 130 (2), 724-731 • DOI: 10.1021/ja077258a

Downloaded from <http://pubs.acs.org> on February 8, 2009



More About This Article

Additional resources and features associated with this article are available within the HTML version:

- Supporting Information
- Links to the 4 articles that cite this article, as of the time of this article download
- Access to high resolution figures
- Links to articles and content related to this article
- Copyright permission to reproduce figures and/or text from this article

[View the Full Text HTML](#)

Competitive Aryl–Iodide vs Aryl–Aryl Reductive Elimination Reactions in Pt(IV) Complexes: Experimental and Theoretical Studies

Anette Yahav-Levi,[†] Israel Goldberg,[†] Arkadi Vignalok,^{*,†} and Andrei N. Vedernikov^{*,‡}

School of Chemistry, The Sackler Faculty of Exact Sciences, Tel Aviv University, Tel Aviv 69978, Israel, and Department of Chemistry and Biochemistry, University of Maryland, College Park, Maryland 20742

Received September 19, 2007; E-mail: avignal@post.tau.ac.il; avederni@umd.edu

Abstract: The platinum(IV) complex *trans*-(dmpe)Pt^{IV}(Ar)₂I₂ (**2**, dmpe = 1,2-dimethylphosphinoethane, Ar = 4-FC₆H₄) rapidly reacts, upon moderate heating in solution under ambient light, via two distinct pathways: isomerization to the corresponding *cis*-isomer (**3**) and Ar–I reductive elimination to give (dmpe)Pt^{II}(Ar)I (**4**). Complex **3** undergoes, upon prolonged heating at high temperatures, an exclusive Ar–Ar reductive elimination reaction to give (dmpe)Pt^{II}I₂. Experimental and DFT studies showed that the **2**-to-**3** isomerization proceeds via three pathways: photochemical or thermal phosphine chelate opening and a mechanism involving cleavage of the Pt–I bond. The isomerization reaction is significantly slowed down but not stopped in the absence of light or in the presence of an excess of tetra-*n*-butylammonium iodide. On the other hand, the Ar–I reductive elimination from **2** proceeds via the Pt^{δ+}–I^{δ-} ion pairlike transition state. Use of the rigid dmpe analogue 1,2-dimethylphosphinobenzene (dmpbz) as the ligand shuts down the chelate ring-opening isomerization pathway and enables faster Ar–I reductive elimination thus making the latter reaction the major reaction route for the dmpbz supported *trans*-diiodo Pt(IV) complex **8**.

Introduction

Examples of a reductive elimination reaction of a carbon–halogen bond from a late transition metal center are scarce compared with the significantly more common carbon–oxygen, carbon–nitrogen, or carbon–carbon bond forming reactions.¹ Usually, the C–X bond formation is less favorable thermodynamically than its microscopic reverse, C–X oxidative addition to a low-valent metal center. Elimination of aryl halides from bulky three coordinate palladium(II) complexes is a rare case of such a reaction that is driven by the steric congestion at the metal center.^{2,3} Several examples of C–X reductive elimination from soluble *high-oxidation state* complexes were also reported. Reductive elimination of iodomethane was observed as one of two competing reactions of (L₂)Pt(R)Me₂I,⁴ and chloromethane was obtained along with methanol in the Shilov methane

oxidation chemistry.⁵ In both cases, the reactions are believed to proceed via the S_N2-type attack of a halide at a Pt(IV)-coordinated methyl group.^{4,6,7} Very recently, the reductive elimination of iodomethane from a Rh(III) center that does not involve an S_N2-type mechanism was reported.⁸ With sp²- and sp-hybridized carbon ligands, the C–X reductive elimination is normally unobserved, especially if the possibility of a more rapid C–C or C–H reductive elimination exists.^{9,10} Thus far, C(sp²)–X reductive elimination was only reported for the chelating carbon ligands and those involving acyclic sp²-carbons.^{11–13} It was also proposed in a Pd-catalyzed intramo-

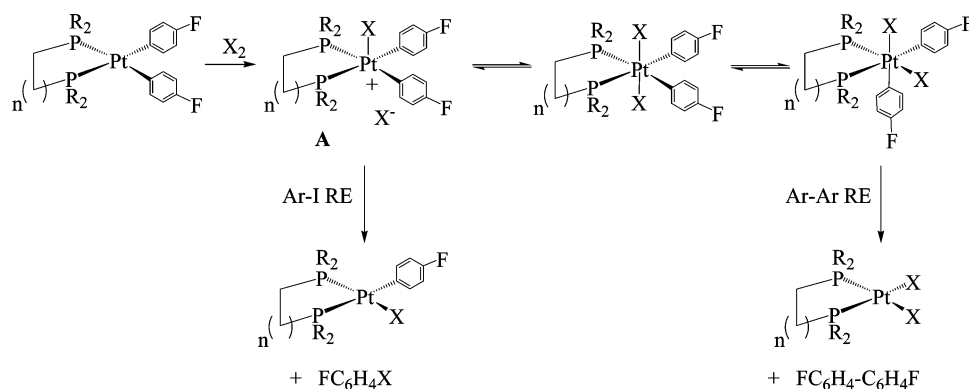
- (5) Shilov, A. E.; Shul'pin, G. B. *Chem. Rev.* **1997**, *97*, 2879.
- (6) (a) Luinstra, G. A.; Wang, L.; Stahl, S. S.; Labinger, J. A.; Bercaw, J. E. *J. Organomet. Chem.* **1995**, *504*, 75. (b) Luinstra, G. A.; Labinger, J. A.; Bercaw, J. E. *J. Am. Chem. Soc.* **1993**, *115*, 3004.
- (7) A similar mechanism was recently proposed for C(sp³)–O reductive elimination in a Pd system: Liu, G.; Stahl, S. S. *J. Am. Chem. Soc.* **2006**, *128*, 7179.
- (8) Frech, C. M.; Milstein, D. *J. Am. Chem. Soc.* **2006**, *128*, 12434.
- (9) Vinyl complexes: (a) Ananikov, V. P.; Mitchenko, S. A.; Beletskaya, I. P. *Russ. J. Org. Chem.* **2002**, *38*, 636. (b) Ananikov, V. P.; Musaev, D. G.; Morokuma, K. *Organometallics* **2001**, *20*, 1652. (c) Ananikov, V. P.; Musaev, D. G.; Morokuma, K. *J. Am. Chem. Soc.* **2002**, *124*, 2839. (d) Ananikov, V. P.; Musaev, D. G.; Morokuma, K. *Organometallics* **2005**, *24*, 715. (e) C(sp²)–C(sp²) reductive elimination is significantly more facile than C(sp³)–C(sp³) reductive elimination: Low, J. J.; Goddard, W. A. *J. Am. Chem. Soc.* **1986**, *108*, 6115.
- (10) Alkynyl complexes: Fuhrmann, G.; Debaerdemaeker, T.; Bauerle, P. *Chem. Commun.* **2003**, 948.
- (11) van Belzen, R.; Elsevier, C. J.; Dedieu, A.; Veldman, N.; Spek, A. L. *Organometallics* **2003**, *22*, 722.
- (12) Alsters, P. L.; Engel, P. F.; Hogerheide, M. P.; Copijn, M.; Spek, A. L.; van Koten, G. *Organometallics* **1993**, *12*, 1831.
- (13) Acyl–X reductive elimination is a key step in the Monsanto methanol carbonylation process: Dekleva, T. W.; Forster, D. *Adv. Catal.* **1986**, *34*, 81.

[†] Tel Aviv University.

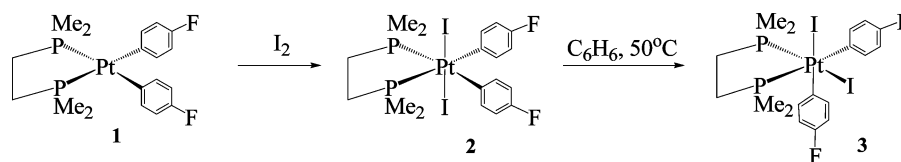
[‡] University of Maryland.

- (1) For general references, see: (a) Collman, J. P.; Hegedus, L. S.; Norton, J. R.; Finke, R. G. *Principles and Applications of Organotransition Metal Chemistry*; University Science Books: Sausalito, CA, 1987. (b) Atwood, J. D. *Inorganic and Organometallic Reaction Mechanisms*, 2nd ed. VCH Publishers: New York, 1997.
- (2) (a) Roy, A. H.; Hartwig, J. F. *J. Am. Chem. Soc.* **2003**, *125*, 13944. (b) Roy, A. H.; Hartwig, J. F. *Organometallics* **2004**, *23*, 1533.
- (3) A recently reported mechanism of Ar–F reductive elimination from a Pd(II) center for the aryl ligand bearing a strong electron-accepting nitro group (a) Yandulov, D. V.; Tran, N. T. *J. Am. Chem. Soc.* **2007**, *129*, 1342) has been contested: (b) Grushin, V. V.; Marshall, W. J. *Organometallics* **2007**, *26*, 4997.
- (4) (a) Goldberg, K. I.; Yan, J.; Winter, E. L. *J. Am. Chem. Soc.* **1994**, *116*, 1573. (b) Goldberg, K. I.; Yan, J.; Breitung, E. M. *J. Am. Chem. Soc.* **1995**, *117*, 6889. (c) Hughes, R. P.; Overby, J. S.; Lam, K.-C.; Incarvito, C. D.; Rheingold, A. L. *Polyhedron* **2002**, *21*, 2357.

Scheme 1



Scheme 2



lecular electrophilic aromatic halogenation,¹⁴ although the reductive elimination step in a Pd(IV) system thus far eluded direct observation. To our knowledge, only one case of an Ar–I reductive elimination from a Pt(IV) center was reported in 1969 and remained the sole example of such a reaction in an aromatic system.^{15,16}

We recently reported that the competitive C–X and C–C reductive elimination reactions take place upon the addition of X₂ (X = I, Br) to a series of diaryl Pt(II) complexes bearing chelating diphosphine ligands.¹⁷ The C–X reductive elimination was proposed to occur from the cationic pentacoordinate Pt(IV) intermediate **A** with the halide ligand occupying the axial position trans to an empty coordination site (Scheme 1). Such a cation is formed during the S_N2-type X₂ oxidative addition to a square planar Pt(II) center.¹⁸ It also can be formed reversibly via the X[−] dissociation from a *trans*-oxidative addition product. Since most of the oxidative addition products, Pt(IV) complexes, are too unstable to be isolated in pure form, no detailed mechanistic studies of C–X reductive elimination could be performed. The only common chelating diphosphine ligand that gave stable Pt(IV) complexes upon I₂ oxidative addition was dmpe (1,2-dimethylphosphinoethane). Here we describe two isomeric complexes *cis*- and *trans*-(dmpe)Pt(Ar)₂I₂ and their dmpbz (dmpbz = 1,2-dimethylphosphinobenzene) analogue that show surprisingly different behavior in C–X reductive elimination.

Results and Discussion

Synthesis of the Diiodo dmpe Pt(IV) Complexes **2** and **3**.

We recently showed that addition of I₂ to the square planar Pt-

(II) diaryl complex **1** results in the clean formation of the *trans*-oxidative addition complex **2** (Scheme 2).¹⁷ This complex can be easily isolated by precipitation with pentane and is reasonably stable at room temperature to be fully characterized by multinuclear NMR techniques. It was also possible to obtain deep red crystals of **2**, suitable for single-crystal X-ray diffraction analysis, by rapid cooling of its CH₂Cl₂–toluene (1:1 ratio) solution at −30 °C. The X-ray structure of **2** (Figure 1a) shows a nearly symmetrical positioning of the pairs of equivalent ligands in the octahedral Pt(IV) complex. The Pt–I1 and Pt–I2 distances of 2.6614(5) and 2.6742(5) Å, respectively, are significantly shorter than the Pt–I distances in the isomeric *cis*-complex **3** (vide supra), where the iodo ligands are located trans to phosphine and aryl ligands that are characterized by a stronger *trans*-influence compared to iodide.¹⁹

Upon heating in benzene or toluene at 50 °C in an oil bath for several hours, complex **2** cleanly converted to the yellow *cis*-isomer **3**, thus confirming that the *trans*-isomer **2** is the kinetic product of oxidative addition of I₂ to square planar Pt(II) complex **1**. Complex **3** has significantly lower solubility in nonpolar solvents than **2** and precipitates readily from the aromatic solvents. Although the crystal structure of **3** was reported (Figure 1b),¹⁷ it was not discussed in detail. In addition to longer Pt–I bonds (2.7077(5) and 2.7848(5) Å for the iodo ligands trans to the phosphine and aryl, respectively) when compared with **2**, the P1–Pt bond of 2.2989(16) Å (trans to the iodine) is significantly shorter than the P2–Pt bond (trans to the aryl group) 2.3892(16) Å. The latter is similar to those observed for **2**, which again correlates well with the *trans*-influences of the three ligands at Pt. Interestingly, very little difference is observed in the Pt–C_{aryl} distances in **3** (2.093(6) and 2.107(6) Å, for aryl groups trans to iodine and phosphorus atoms, respectively). Also, the P1–Pt–P2 bond angles for complexes **2** and **3**, of 84.48(7)° and 85.59(6)°, respectively, are very similar.

C–C Elimination from Complex **3.** Heating complex **3** at 85 °C in toluene resulted in a slow reaction to cleanly give

(14) (a) Fahey, D. R. *J. Organomet. Chem.* **1971**, *27*, 283. (b) Kalyani, D.; Dick, A. R.; Anani, W. Q.; Sanford, M. S. *Tetrahedron* **2006**, *62*, 11483–11498. (c) Kalyani, D.; Dick, A. R.; Anani, W. Q.; Sanford, M. S. *Org. Lett.* **2006**, *8*, 2523–2526.

(15) (a) Ettore, R. *Inorg. Nucl. Chem. Lett.* **1969**, *5*, 45. (b) In our hands, the reaction appeared to be more complex giving large amounts of a byproduct.

(16) We very recently observed facile Ar–I reductive elimination that occurs upon the reaction of Pd(II) complexes with XeF₂: Kaspi, A.; Yahav-Levi, A.; Goldberg, I.; Vignalok, A. *Inorg. Chem.*, published online Dec. 4, 2007 <http://dx.doi.org/10.1021/ic701722f>.

(17) Yahav-Levi, A.; Goldberg, I.; Vignalok, A. *J. Am. Chem. Soc.* **2006**, *128*, 8710.

(18) Kubota, M.; Boegeman, S. C.; Keil, R. N.; Webb, C. G. *Organometallics* **1989**, *8*, 1616.

(19) For a recent review, see: Coe, B. J.; Glenwright, S. J. *Coord. Chem. Rev.* **2000**, *203*, 5.

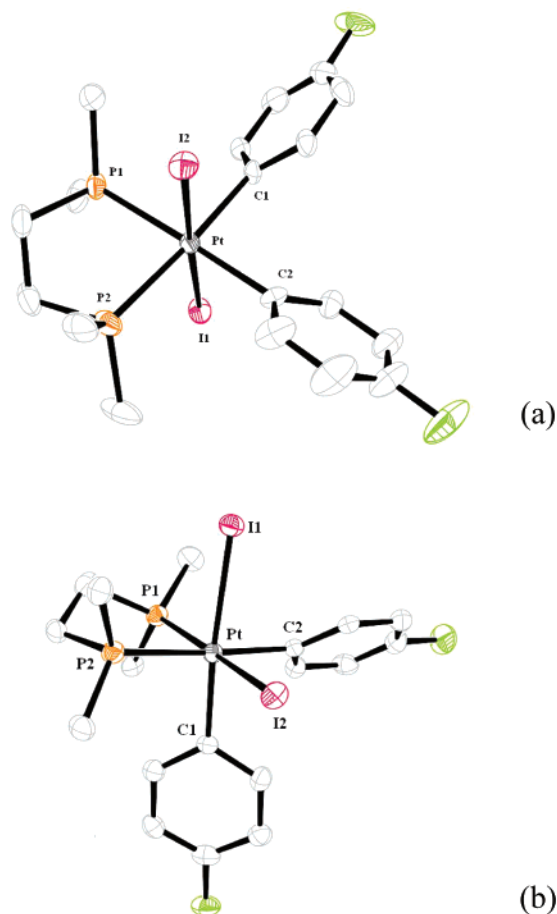
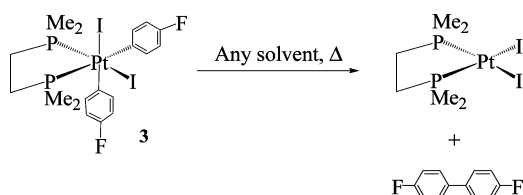


Figure 1. X-ray crystal structure of complexes 2 (a) and 3 (b).

Scheme 3

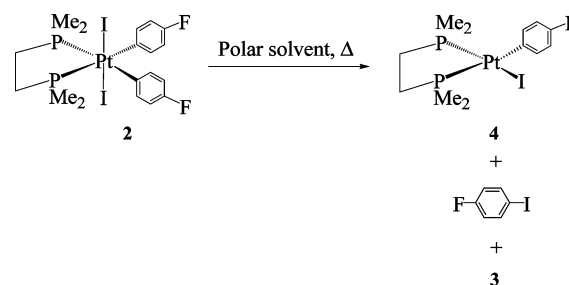


products of C–C reductive elimination, the biaryl (4-FC₆H₄)₂ and (dmpe)Pt(I)₂ (30% conversion after 25 h, Scheme 3). Clean aryl–aryl reductive elimination from 3 was also observed in more polar solvents, such as THF or DMF; the reaction rates were faster than that using toluene (50% conversion after 25 h at 85 °C in DMF). The biaryl elimination in DMF was inhibited in the presence of 10 equiv of tetra-*n*-butyl ammonium iodide (TBA-I) (30% conversion after 40 h at 85 °C) so suggesting that the reaction might proceed via a five-coordinate cationic intermediate resulting from iodide ion dissociation from 3. In aromatic hydrocarbon solutions, where formation of free ions is unlikely, the C–C elimination could proceed via ion pairs and/or via the five-coordinate transient resulting from the chelate ring opening, (η^1 -dmpe)PtAr₂I₂.

C–I Elimination vs Thermal Isomerization of Complex 2. Surprisingly, when DMF or THF, solvents more *polar* than benzene or toluene, were used, *trans*-diiodo complex 2 formed products of C–I reductive elimination, (dmpe)Pt(Ar)I (4) and 4-FC₆H₄I, along with the *cis*-diiodo complex 3 (Scheme 4).

Since 3 is essentially stable under the reaction conditions, we initially attributed the formation of 4 and 4-FC₆H₄I to the

Scheme 4



mechanism in which the cationic intermediate 5 and/or ion pairs [5]⁺I[−] form in DMF (Scheme 5).

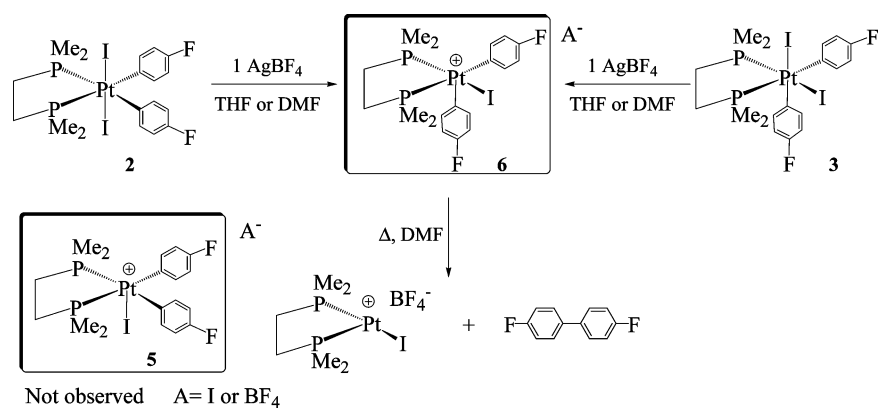
Five-coordinate cation 5 (A = I), resulting from the iodide dissociation from 2, is expected to be prone to isomerization to, more stable thermodynamically, cation 6 (A = I). Lower stability of 5 vs 6 may originate from an unfavorable *trans*-influence exerted by both aryl groups on the Pt–P bonds. In turn, the *trans*-influence of the iodo ligand in 6 is much weaker.¹⁹ Indeed, attempts to generate 5 (presumably, along its DMF- or THF-solvate) in the form of a tetrafluoroborate salt by reacting 2 with AgBF₄ in THF or DMF resulted in the instantaneous formation of cation 6 (A = BF₄), *without* noticeable C–I reductive elimination. Complex 6 (A = BF₄) was also prepared by reacting 3 with AgBF₄. Based on these observations, we suggest that 5 and 6 are potential intermediates involved in the isomerization of 2 to 3 in polar DMF.

The fact that both 4 and 3 formed from 2 in DMF at comparable rates could be assigned to the involvement of both ion 5 and derived ion pairs [5]⁺I[−] that are prone to C–I elimination rather than isomerization, in contrast to 5 itself. The involvement of an ion-pair-like transition state instead of ion pairs [5]⁺I[−] could not be excluded either.

Upon heating, 6 produced the biaryl (4-FC₆H₄)₂ and (dmpe)Pt(I)BF₄ (*t*_{1/2} = 1.5 h in DMF at 60 °C) (Scheme 5). The latter complex was prepared independently from (dmpe)Pt(I)₂ and AgBF₄. The rate of the biaryl elimination from 6 was faster than that from 3 under the same conditions (*t*_{1/2} = 25 h in DMF at 85 °C).

Photochemical and Thermal Isomerization of Complex 2 to Complex 3. Although the general reactivity patterns of 2 in *polar* solvents were reproducible, the ratio between 3 and 4 varied noticeably even when the reaction was run under seemingly identical conditions. Even more unexpectedly, heating samples of 2 in DMF inside the NMR probe gave 3/4 ratios that were different from those obtained in an oil bath under the bright light of a 100 W incandescent lamp at the same temperatures (see Table 1 for rate constants of isomerization, *k*_{isom}, and reductive elimination reaction, *k*_{RE}, entries 1 and 2). Very slow formation of 4 and the iodoarene was also observed in *nonpolar* benzene when the reaction was set up inside an NMR probe (entry 5), although normally no such products were observed in this solvent when the reaction was set up under light in an oil bath (entry 6). Influence of an external magnetic field aside, this observation suggested that the reactivity of 2 depends on the presence of light. Addition of 1 equiv of BHT did not result in significant changes in the reactivity, suggesting that no free radicals are formed in the reaction. Interestingly, addition of 10 equiv of TBA-I to a reaction mixture in DMF exposed to an ambient light slowed down the rate of disap-

Scheme 5



Scheme 6

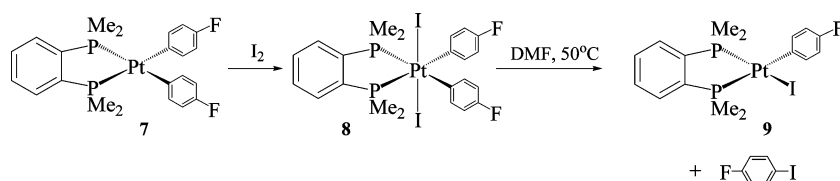


Table 1. Kinetic Data for Conversion of Complexes **2** and **8** under Various Reaction Conditions including the Presence (Oil Bath, 100 W Incandescent Lamp) and Absence of Light (inside an NMR Probe)

compd	solvent	<i>t</i> , °C	light conditions and TBA-I	<i>t</i> _{1/2} (<i>cis</i> -Pt ^{IV} /Pt ^{II} ratio)	<i>k</i> _{isom} × 10 ³ , min ⁻¹	<i>k</i> _{RE} × 10 ³ , min ⁻¹
1	DMF	60	dark	80 min (1:4)	1.7	7
2			light	25 min (2:1)	18	9
3			light with TBA-I	60 min (1:2.5)	3.3	8
4	benzene	60	dark with TBA-I	80 min (1:4)	1.7	7
5			dark	9 h (9:1)	1.2	0.1
6			light	2.5 h (1:0)	4.6	0
7	DMF	50	light with TBA-I	4 h (1:0)	2.9	0
8			dark	30 min (0:1)	0	23
9			light	30 min (0:1)	0	23
10	DMF	30	dark	6 h (0:1)	0	1.9
11		40	dark	75 min (0:1)	0	9.2
12		60	dark	4 min (0:1)	0	173

pearance of **2** more than twice (entry 3), affecting *k*_{isom} but not *k*_{RE} and leaving the Ar–I reductive elimination process as the major reaction pathway. Similarly, compared to the reaction setup in benzene under light (entry 6) the addition of 10 equiv of TBA-I decreased the rate constant *k*_{isom} noticeably (entry 7).

At the same time, for the dark reaction in DMF the addition of 10 equiv of TBA-I did not affect the magnitude of *k*_{isom} and *k*_{RE}; both C–I elimination and isomerization of **2** to **3** were observed (entries 1 and 4).

Remarkably, as it follows from Table 1, the rate constant of C–I elimination from **2** in DMF, *k*_{RE}, remained approximately unchanged in the presence of light or TBA-I, whereas the rate constant of isomerization of **2** to **3**, *k*_{isom}, was affected by both TBA-I and light. Importantly, the magnitude of *k*_{isom} in DMF remained significant even in the dark suggesting that at least two mechanisms of isomerization were operative, a photochemical and a thermal one.

We suggest that in the cases of both thermal and photochemical isomerization reaction the mechanisms include conversion of **2** to low-coordinate transients. Light might facilitate a ligand dissociation from a Pt center via either loosening the Pt–I bond²⁰ or promoting a chelate ring-opening.²¹ The latter process was

proposed for Pt(IV) iodo complexes bearing a chelating ethylene diamine ligand. A thermal ring-opening was also reported in the reductive elimination chemistry of Pt(IV), not assisted by light.²²

Finally, the C–I reductive elimination in both benzene and DMF might proceed via ion pairs or an ion-pair-like transition state.

Synthesis of the Diiodo dmpbz Pt(IV) Complex 8: C–I Reductive Elimination. To verify that the diphosphine chelate opening might be responsible for the thermal and/or photochemical *trans*-to-*cis* rearrangement process, we prepared a more rigid analogue of **1**, (dmpbz)Pt(Ar)₂ complex **7** (dmpbz = 1,2-

- (20) (a) Bryan, S. A.; Dickson, M. K.; Roundhill, D. M. *J. Am. Chem. Soc.* **1984**, *106*, 1882. (b) Bryan, S. A.; Dickson, M. K.; Roundhill, D. M. *Inorg. Chem.* **1987**, *26*, 3878. (c) Cross, R. J.; Davidson, M. F. *J. Chem. Soc., Dalton Trans.* **1987**, 139. (d) Appleton, T. G.; Berry, R. D.; Hall, J. R.; Neale, D. W. *J. Organomet. Chem.* **1988**, *342*, 399. (e) Rich, R. L.; Taube, H. *J. Am. Chem. Soc.* **1954**, *76*, 2608.
- (21) (a) Kratochwil, N. A.; Guo, Z.; del Socorro, Murdoch, P.; Parkinson, J. A.; Bednarski, P. J.; Sadler, P. J. *J. Am. Chem. Soc.* **1998**, *120*, 8253. (b) Kratochwil, N. A.; Ivanov, A. I.; Patriarca, M.; Parkinson, J. A.; Gouldsworthy, A. M.; del Socorro Murdoch, P.; Sadler, P. J. *J. Am. Chem. Soc.* **1999**, *121*, 8193.
- (22) (a) Crumpton-Bregel, D. M.; Goldberg, K. I. *J. Am. Chem. Soc.* **2003**, *125*, 9442. (b) Crumpton, D. M.; Goldberg, K. I. *J. Am. Chem. Soc.* **2000**, *122*, 962.

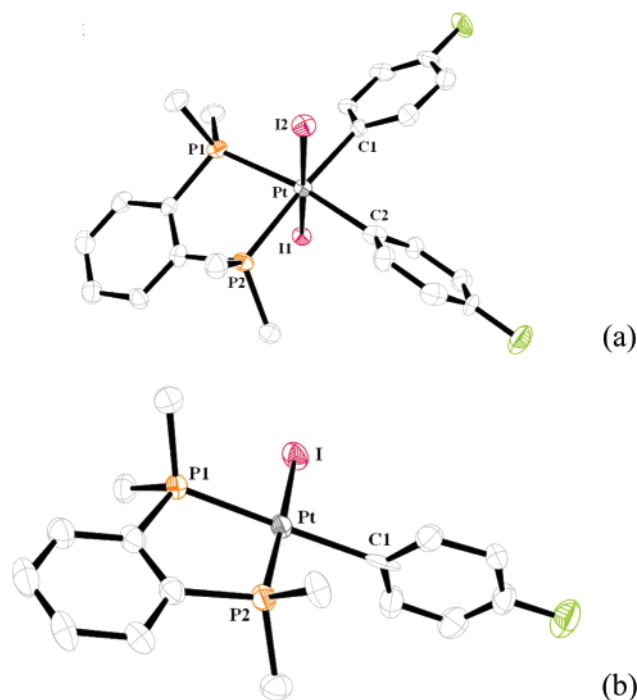


Figure 2. X-ray crystal structure of complexes **8** (a) and **9** (b).

dimethylphosphinobenzene),²³ and reacted it with I₂. The *trans*-diiodo Pt(IV) complex **8** was obtained in a quantitative yield (Scheme 6) and fully characterized, including X-ray diffraction analysis. Importantly, the crystal structure of **8** showed nearly identical bond lengths with those in **2** (Figure 2a). The P1–Pt–P2 bond angles for both complexes are also very similar, 82.56(7)° vs 84.48(7)°, in **8** and **2**, respectively. Mild heating of this complex in DMF both in the dark (entry 8) and under light (entry 9) gave exclusively the products of C–I reductive elimination, 4-FC₆H₄I and Pt(II) complex **9** which was characterized by X-ray diffraction analysis (Figure 2b). No effect of light on this reaction was observed. Furthermore, addition of 10 equiv of TBA-I did not affect the C–I reductive elimination rate in DMF.

Therefore, as in the case of analysis of the reactivity of **2**, we can conclude that the C–I reductive elimination does not involve formation of a dmpbz analogue of ion **5** as a result of iodide dissociation from **8**. These observations can be accounted for if C–I elimination occurs from ion pairs or via an ion-pair-like transition state as it was assumed for complex **2**.

To shed light on the reaction mechanism, the activation parameters of the C–I reductive elimination from **8** in DMF were determined using the NMR technique (Table 1, entries 8, 10–12). Kinetic experiments showed that the reaction is first-order in complex **8** with $\Delta H^\ddagger = 29.11 (\pm 0.12)$ kcal/mol and $\Delta S^\ddagger = 15.98 (\pm 0.46)$ cal/(mol·K) (Figure 3). The relatively high activation enthalpy might be indicative of the significant Pt–C and Pt–I bond weakening in the transition state. The relatively high positive value of the activation entropy also suggests the disorder increase in the transition state. The activation parameters are consistent with the idea of direct elimination from a six-coordinate Pt(IV) complex via an ion-pair-like transition state if the charge separation in the transition state is not very different

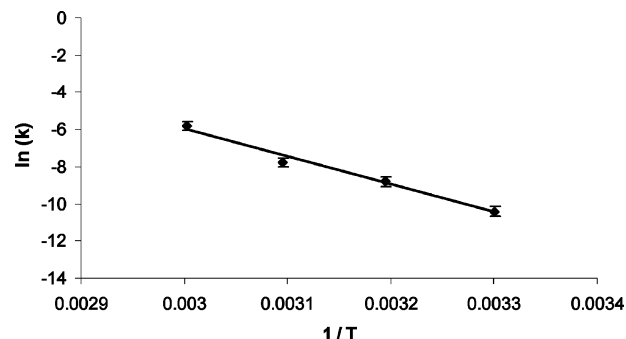
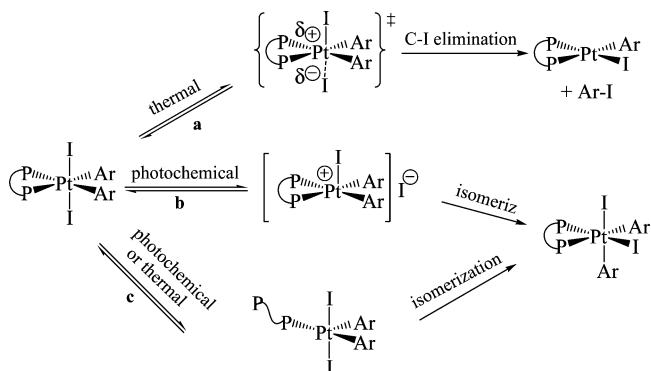


Figure 3. Eyring plot of the 4-FC₆H₄I reductive elimination from **8** in DMF.

Scheme 7



from that in **8**. In contrast, a significant charge separation increase in the transition state might induce the solvent electrostriction, cause the entropy loss, and invert the sign of the C–I elimination activation entropy.²⁴

Mechanisms of C–I Elimination and Isomerization of **2 and **8****. It is important to emphasize the difference between the mechanism of Ar–I reductive elimination from **2** or **8** and that for the CH₃–I reductive elimination reaction from diphosphine Pt(IV) iodo trimethyl complexes reported earlier.⁴ In the latter case, as well as the mechanistically similar CH₃–OR reductive elimination reactions,^{4,25} the presence of an external nucleophile is essential to achieve an S_N2-type attack at a Pt(IV)-coordinated C(sp³) center. In complexes **2** and **8** the aryl ligand is not as susceptible to external attacks by nucleophiles as the methyl group in LPtMe₃I. C–I reductive elimination from **2** and **8** can be viewed as a microscopic reverse of the concerted oxidative addition of aryl halides to a low valent metal center. In addition, the presence of two aryl ligands allows for competition between the Ar–I and Ar–Ar reductive elimination reactions, the outcome of which is dependent on the metal complex geometry.²⁶

Our view of plausible mechanisms of competing isomerization and C–I reductive elimination reaction involving complexes **2** and **8** is summarized in Scheme 7.

As it follows from previous discussion, the C–I elimination in our systems is a thermal-only reaction which is not affected

(23) For the ligand synthesis see: Kang, Y. B.; Pabel, M.; Pathak, D. D.; Willic, A. C.; Wild, S. B. *Main Group Chem.* **1995**, *1*, 89.

(24) Tobe, M. L.; Burgess, J. *Inorg. React. Mech.*, 2nd ed.; Prentice Hall: New York, 2000.

(25) (a) Williams, B. S.; Goldberg, K. I. *J. Am. Chem. Soc.* **2001**, *123*, 2576. (b) Williams, B. S.; Holland, A. W.; Goldberg, K. I. *J. Am. Chem. Soc.* **1999**, *121*, 252. (c) Vedernikov, A. N.; Binfield, S. A.; Zavalij, P. Y.; Khusnutdinova, J. R. *J. Am. Chem. Soc.* **2006**, *128*, 82. (d) Khusnutdinova, J. R.; Zavalij, P. Y.; Vedernikov, A. N. *Organometallics* **2007**, *26*, 3466.

(26) Ruddick, J. D.; Shaw, B. L. *J. Chem. Soc. A* **1969**, 2969.

by light and might proceed via an ion-pair-like transition state in a DMF or benzene solution at elevated temperatures (Scheme 7, path a). The ability of a metal complex to undergo a reductive elimination reaction is a function of a number of factors: electron density of the metal center, ligand steric interactions, the presence of coordination vacancies, the configuration of the metal center.¹ Since **2** and **8** are structural analogues, two latter factors can be considered identical for both complexes. Noteworthy, dmpbz is not only a more rigid ligand but also expected to be a poorer electron donor compared to dmpe as follows from the IR data for similar LNi(CO)₂ complexes with L = (Et₂PCH₂)₂ and (Et₂P)₂-*o*-C₆H₄.²⁷ Therefore, C–I elimination from **8** containing the rigid electron poorer dmpbz is expected to be faster than that from **2**. This consideration is consistent with our observations: C–I elimination from **8** in DMF at 60 °C is about 25 times more rapid than that from **2** under the same experimental conditions (Table 1, entries 1 and 12). Correspondingly, the ion-pair-like transition state for C–I elimination is expected to be more reagent-like and therefore lower in energy in the case of dmpbz complex **8**.

The ability of an octahedral 18-electron complex to undergo isomerization might be a function of its ability to produce a five-coordinate transient.^{25a} As experiments with complex **2** and AgBF₄ show, “free ion” **5**, or more likely a loose ion pair or a solvento complex formed by **5**, is most probably involved in an isomerization reaction in DMF. Since this reaction channel is suppressed by additives such as TBA-I and is in the dark, it might include a photochemical Pt–I bond ionization (Scheme 7, path b). Path b is higher in energy in less polar solvents and most likely will be suppressed in nonpolar benzene. More electron-poor complex **8** will be less prone to produce five-coordinate cations compared to **2**.

Another way to produce a five-coordinate transient involved in an isomerization reaction is by chelate ring-opening in **2** or **8** (Scheme 7, path c). Since in the case of complex **2** the isomerization is observed under both dark and light conditions in DMF and benzene solutions, both thermal and photochemical ring-opening paths might be operative here. In turn, photochemical and thermal chelate ring-opening are expected to be more facile in **2** compared to more rigid **8**. Accordingly, in contrast to **2**, complex **8** demonstrated the absence of isomerization behavior in DMF.

Based on the analysis given above, complex **8** is less prone to isomerization than **2**. In turn, **8** is more prone to C–I elimination. Therefore, the ratio of products of C–I elimination/isomerization products will be higher for **8** compared to **2** under identical reaction conditions, which was observed experimentally.

Computational Modeling of Reactivity of 2, 5, and 8. To get a better understanding of the behaviors of complexes **2** and **8** in reductive elimination and isomerization reactions, a DFT study was undertaken. The primary questions to answer were as follows:

- (1) How facile is direct C–I elimination from **2** and **8**?
- (2) How facile is thermal chelate ring opening in complexes **2** and **8**?
- (3) How facile is photochemical chelate ring opening in complexes **2** and **8**?

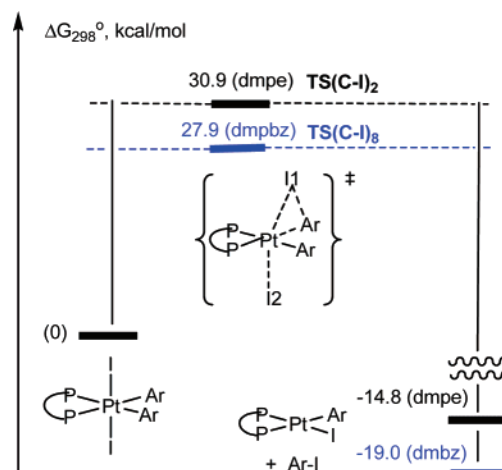


Figure 4. Standard Gibbs energy changes for 4-IC₆H₄F elimination from complexes **2** and **8**, kcal/mol.

(4) How competitive are isomerization and C–I elimination reactions of five-coordinate transients resulting from the chelate ring opening in complexes **2**, **8** and from iodo ligand abstraction, cation **5**?

DFT Modeling: C–I Elimination from 2 and 8. A diagram given in Figure 4 shows that the activation barrier for 4-fluoroiodobenzene elimination from complex **2** is 3.0 kcal/mol higher for ($TS(C-I)_2$ vs $TS(C-I)_8$) and the reaction energy is 4.2 kcal/mol lower compared to complex **8** stabilized by dmpbz. These results are consistent with the observed difference in reactivity of **2** and **8** in the C–I elimination reaction. According to data in Table 1, under the same conditions, k_{RE} for **8** is significantly higher than k_{RE} for **2** in DMF. The experimentally found Gibbs activation energy for C–I elimination from **8** in DMF is 26.4 kcal/mol, a reasonable match of the calculated 27.9 kcal/mol. As it follows from the calculated Pt–I2 bond length, 3.107 Å in $TS(C-I)_8$ vs 2.743 Å in **8**, and 3.306 Å in $TS(C-I)_2$ vs 2.740 Å in **2**, the ion-pair character of the transition state $TS(C-I)_8$ is less pronounced than that for $TS(C-I)_2$. Consistent with that result, a more electron-rich metal center in **2** should acquire a greater positive charge in the course of Pt–I2 bond ionization and elongation to eliminate the Ar–I. The results in Figure 4 are consistent with available experimental observations showing significantly higher reactivity of **8** in C–I elimination compared to **2**.

In support of the idea of an ion-pair-like character of $TS(C-I)$'s, it is worth comparing the experimentally determined and DFT calculated values of entropy of activation of C–I elimination from **8**, $\Delta S^\ddagger(\mathbf{8})$. The calculated gas-phase entropy of activation is 4.1 cal/(K·mol) which is positive, similar to the experimentally found entropy of activation in DMF solution, 16.0 cal/(K·mol). If elimination occurs from contact or solvent separated ion pairs where ions experience strong interactions with solvent, solvent electrostriction might diminish significantly the magnitude and even change the sign of $\Delta S^\ddagger(\mathbf{8})$ that is expected to be positive in the absence of such effects.²⁴ The calculated dipole moments of **2**, **8**, $TS(C-I)_2$, and $TS(C-I)_8$ are very similar: 11.5 D (**2**), 11.2 D ($TS(C-I)_2$), 12.4 D (**8**), and 11.3 D ($TS(C-I)_8$) suggesting that the ion-pair-like character of these $TS(C-I)$'s is not very pronounced and that solvent effects should not alter dramatically the reaction entropy of activation.

(27) Chatt, J.; Hart, F. A. J. *Chem. Soc.* **1960**, 1378.

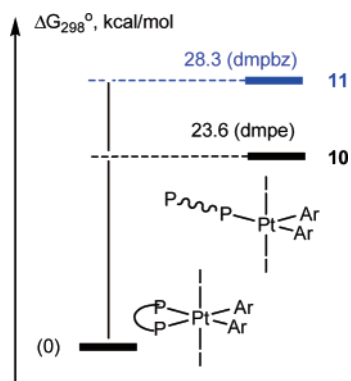


Figure 5. Standard Gibbs energy changes for thermal chelate ring opening in complexes **2** and **8**, kcal/mol.

DFT Modeling: Thermal Ring Opening in 2 and 8. A chelate ring opening in complexes **2** and **8** to produce five-coordinate η^1 -diphosphine species requires 23.6 kcal/mol (intermediate **10**) and 28.3 kcal/mol (intermediate **11**), respectively (Figure 5). Assuming that the barrier of ring opening is approximately the same as the reaction energy, the ring opening can occur at a slow rate already at 25 °C for complex **2** with $t_{1/2} = 6.4$ h which corresponds to $\Delta G_{298}^\ddagger = 23.6$ kcal/mol, according to the Eyring equation, whereas for complex **8** a comparable rate is expected at 80 °C ($t_{1/2} = 8.9$ h) only. Therefore, as compared to **8**, **2** is much more efficient in producing five-coordinate transient (η^1 -L)PtAr₂I₂ via thermal chelate ring opening.

DFT Modeling: Photochemical Ring Opening in 2 and 8. Time-dependent DFT calculations allowed us to determine the energy and light wavelength necessary for the lowest-energy electronic excitation in **2** and **8**,²⁸ 39.3 kcal/mol (727 nm) for the dmpe complex and 37.8 kcal/mol (757 nm) for the dmpbz complex. In both complexes the HOMO is a π -bonding orbital localized mostly on 12 carbon atoms of two 4-fluorophenyl ligands, whereas the LUMO is the σ -I–Pt–I antibonding orbital. Correspondingly, the triplet species ³[**2**] and ³[**8**] having singly occupied σ -I–Pt–I antibonding orbitals are characterized by significantly elongated Pt–I bonds. For instance, the Pt–I bond length in ³[**2**] is 3.200 Å vs 2.740 Å in ¹[**2**]. Assuming that excited-state species should be long-lived enough to exhibit chelate ring opening or other reactivity, we considered as such the lowest energy triplet states of **2** and **8**, ³[**2**] and ³[**8**], respectively. These triplets could be produced as a result of spin interconversion of singlet excited states of complexes **2** and **8**. The ring opening in ³[**2**] and ³[**8**] followed by another spin interconversion might lead then to singlet transients **10** and **11**, respectively. Altogether, these photoassisted transformations might constitute an alternative path to produce five-coordinate intermediates **10** and **11**.

In fact, for both ³[**10**] and ³[**11**] the stationary point corresponding to ³[*trans*-(η^1 -L)PtAr₂I₂] could not be located. Instead, all our geometry optimization attempts led to isomeric products,³-[*cis*-(η^1 -L)PtAr₂I₂], ³[**12**] for dmpe and ³[**13**] for dmpbz. Therefore, the ring opening in ³[**2**] and ³[**8**] was accompanied with I–Pt–I angle change and isomerization. The energy required for the chelate opening in ³[**2**] to produce five-coordinate triplet ³[*cis*-(η^1 -dmpe)PtAr₂I₂] is 10.7 kcal/mol only, whereas ³[*cis*-(η^1 -dmpe)PtAr₂I₂] is 17.6 kcal/mol in the case of

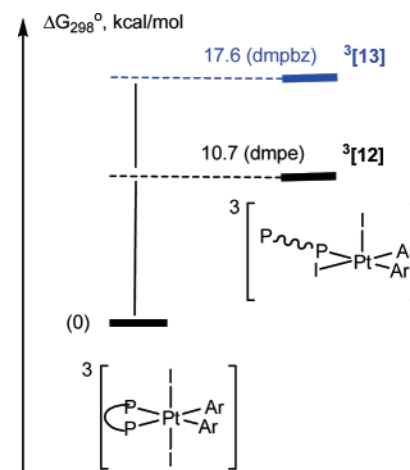


Figure 6. Standard Gibbs energy changes for chelate ring opening and isomerization in ³[**2**] and ³[**8**], kcal/mol.

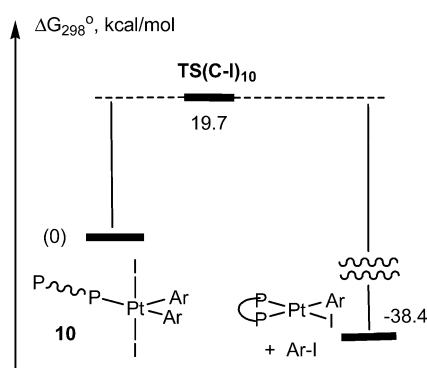


Figure 7. Standard Gibbs energy changes for Ar–I elimination from **10**, kcal/mol.

³[**8**] (Figure 6). Thus, the light-induced chelate ring opening in **2** and **8** may be an effective pathway to isomerization of these species. Considering this, we assume that the light intensity is sufficient to make these reactions fast enough.

DFT Modeling: Isomerization and C–I Elimination Reactions of Five-Coordinate Transient 10. The calculated barrier for the C–I reductive elimination from five-coordinate transient **10** is 19.7 kcal/mol (Figure 7; TS(C–I)₁₀), too high to allow for the thermal chelate ring opening of **2** (23.6 kcal/mol; Figure 5) with subsequent C–I elimination in a thermal reaction at temperatures not exceeding 85 °C used in this work.

All our attempts to locate the transition state for isomerization of **10** to **12** failed, presumably because of the relative flatness of the corresponding potential energy surface. Still, available computational estimates of the energy of species with the I–Pt–I angle varying between $\sim 180^\circ$ (**10**) and $\sim 90^\circ$ (**12**) suggest that the reaction barrier does not exceed 6 kcal/mol, low enough to allow for thermal isomerization of **2** via five-coordinate transient **10**. This suggestion is consistent with our experimental observations of the ability of **2** to undergo isomerization in the dark.

DFT Modeling: Isomerization and C–I Elimination Reactions of Cations 5 and 6. Complete removal of the iodide anion from **2** which leads to cation **5** will increase electron deficiency of the metal and, consistent with the results of our computational analysis of C–I elimination (Figure 4), will lower the barrier of C–I reductive elimination from the Pt(IV) center. Indeed, the barrier height calculated for the gas-phase cation **5**

(28) JAGUAR, version 7.0; Schrodinger Inc.: Portland, OR, 2007.

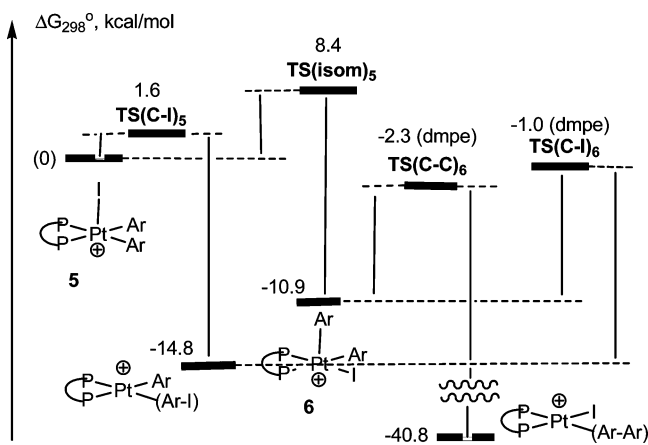


Figure 8. Standard Gibbs energy changes for isomerization, C–C and C–I reductive elimination from cations **5** and **6**, kcal/mol.

is 1.6 kcal/mol only (Figure 8; **TS(C–I)₅**). With the activation barrier for isomerization of **5** to **6** being 8.4 kcal/mol (**TS(isom)₅**), the C–I elimination is a much faster reaction. No low barrier C–C reductive elimination from cation **5** can be expected since that reaction would lead to a nonplanar (dmpe)PtI(ArI)⁺ complex with the iodide ligand in the axial position, a highly unfavorable configuration for a d⁸ metal complex.

In turn, **6** which is 10.9 kcal/mol more stable than **5**, based on our DFT calculations, can undergo fast C–C elimination with a Gibbs activation energy of 8.6 kcal/mol (**TS(C–C)₆**) and slower C–I elimination with a higher activation barrier of 9.9 kcal/mol (**TS(C–I)₆**). With regard to the difference in the barrier heights, the gas-phase values given in Figure 8 should be used with caution when applied to the analysis of reactivity of [**5**]₂BF₄ in solution. The presence of a counterion significantly increases the barrier of the C–I elimination reaction, as follows from the comparison of data in Figures 4 and 8. In support of this statement, using DFT modeling we found that the barrier for C–I elimination from a contact ion pair **5**(κ^1 -F-BF₄) is 10.7 kcal/mol, about 9 kcal/mol higher than that for **5**. Similar is the effect of a coordinated polar solvent molecule, such as DMF. The DFT calculated barrier for C–I elimination from solvento-complex **5**(κ^1 -O-DMF)⁺ is 9.5 kcal/mol, an about 8 kcal/mol increase compared to **5**. In addition, ion association and solvent coordination in DMF solution would affect the rate of isomerization of **5** to **6**. Its correct computational analysis would require consideration of solvent effects which was not done in this work. Therefore, because of the presence of strong solvent–counterion–cation interactions that are not taken into account in our

computational model illustrated in Figure 8, we cannot predict the relative height of barriers for C–I elimination and isomerization of cation **5** associated with BF₄[−] or DMF in DMF solutions. Solvent effect might also be important in the photochemically induced formation of **5** (path b, Scheme 7), which could not be properly assessed. At the same time, our calculations of the reactivity of the more stable cation **6** are fully consistent with our experimental observations. Only C–C bond formation can take place in this case, although the difference in the kinetic barriers for both reductive elimination reactions is not large.

Conclusion

In conclusion, we demonstrated that aryl–halide reductive elimination can occur in Pt(IV) complexes under very mild conditions. Although the complete mechanistic picture is complicated, it is clear that the complex geometry plays a crucial role in determining the reaction outcome. The less thermodynamically stable trans-complex **2** can undergo a facile Ar–I reductive elimination reaction. Maintaining this configuration is essential for the formation of a carbon–halogen bond, as the more stable cis-isomer **3** gives exclusively the products of C–C reductive elimination, albeit under much harsher conditions. Unlike the Ar–I elimination, which takes place in a single path, the competing trans/cis isomerization reaction can proceed via several pathways, thermal and photochemical. Thus, solvent, light, and choice of ligand can influence the competition. The use of the rigid and electron-poorer dmpbz analogue of dmpe allowed for significant discrimination of these competing reactions by rate, with the Ar–I reductive elimination becoming the major reaction path. The kinetic analysis, supported by the DFT calculations, showed that this reaction occurs via an ion-pair-like, late transition state. Noteworthy, while the formation of an aryl–iodide bond gives relatively little energy gain in these systems, especially compared with the competitive Ar–Ar reductive elimination (−14.8 kcal/mol vs −40.8 kcal/mol), the reaction is kinetically driven and irreversible.

Acknowledgment. This work was supported by a Tel Aviv University Internal Grant to A.V. and by the US-Israel Binational Science Foundation.

Supporting Information Available: Experimental and computational details (PDF); X-ray crystal data for complexes **2**, **3**, **8**, and **9** (CIF). This material is available free of charge via the Internet at <http://pubs.acs.org>.

JA077258A